WILEY | Hindawi

Research Article

A Case Study of Deep DNAPL Contamination in Marine Soft Clays

Yanbin Gao [ID],[1] **Wenqi Ji,**[2] **and Tao Li**[3]

[1]Department of Geotechnical Engineering, Tongji University, 1239 Siping Road, Shanghai, China 200092
[2]Hatch Ltd., Dynamic Earth Solutions (DES), 2699 Speakman Drive, Mississauga, Ontario, Canada L5K 1B1
[3]SGIDI Engineering Consulting (Group) Co., Ltd., Shanghai, China 200433

Correspondence should be addressed to Yanbin Gao; yanbin_gao@tongji.edu.cn

Aquifers in China's southeast coastal areas are protected by the overlying marine soft clays formed in Holocene transgression. However, a fundamental understanding of the characteristics of DNAPL (dense nonaqueous phase liquid) contamination in marine soft clays is limited. The study was conducted on the site of a former pharmaceutical factory in Shanghai, where serious 1,1,2-trichloroethane (DNAPL) contamination was detected up to the depth of 22.0 m below the existing grade. Partitioning calculation method was used to identify the presence of pure phase, and the results showed that pure 1,1,2-trichloroethane was accumulated at the interface of the upper soft silty clay and lower soft clay. The vertical transport was believed to be the pure DNAPL displacing pore water following the principle of two-phase flow, rather than the convection and diffusion of aqueous phase. The contamination (NAPL-soil interaction) impacted the soil properties slightly, and this effect could not account for the deep contamination. Soil structure analysis showed that these clays contained a proportion of large interaggregate pores, providing pathways for the transport of pure DNAPL. Considering their flocculated structure, the marine soft clays are not capable to perform as a barrier to prevent the downward migration of pure DNAPL.

1. Introduction

Soil and groundwater contamination due to leaks and spills of toxic organic chemicals has been well acknowledged. The organic components contaminate the subsoils and groundwater in the form of slightly soluble and/or volatile nonaqueous phase liquids (NAPLs), as a result of pipeline breaks, poor storage, and/or disposal practices, such as leaking of underground storage tanks, or as a solute dissolved in water as in the case of landfill leachate [1]. Dense nonaqueous phase liquids (DNAPLs), including chlorinated solvents (most commonly trichloroethene and chlorobenzene) and polychlorinated biphenyls (PCB), are commonly found as contaminants in the subsoils and groundwater due to their intensive use in the industry. As DNAPLs have a larger density than that of water, they can transport downward through the vadose zone and/or saturated zone until encountering a barrier, e.g., a competent clay or bedrock surface. A few decades ago, clay-rich deposits were assumed to be a barrier to protect the underlain aquifers

from DNAPL contamination due to their lower void ratio (e.g., [2, 3]). However, in North America where many aquifers were protected by the overlying clayey or silty aquitards, DNAPL contaminants were often found in the confined aquifers, through preferential pathways such as open fractures, root holes, stratigraphic windows, or unsealed boreholes [4–6]. Roberts et al. [7] and Schwartz et al. [8] had reported a transformer manufacturing plant site in Regina, Saskatchewan, Canada, where the spilled polychlorinated biphenyl (PCB) migrated laterally in a perched groundwater regime and moved downward through the fractures in the unsaturated Regina clay to the depth of 7.0 m-9.0 m below grade. PPG Industries [9] reported the migration of tetrachloroethylene (PCE) and trichlorethylene (TCE) DNAPLs through a 50.0 m thick alluvial clay aquitard to the underlying aquifer at the site of a chemical manufacturing facility, due to the root holes and fractures acting as preferential pathways for DNAPL migration. Fjordbøge et al. [10] reported a site of a former distribution facility for tetrachloroethene (PCE) and TCE located in Naverland near

Copenhagen, Denmark, where the vertical migration of DNAPL occurred through fractures in a shallow oxidized zone. In these cases, fractures were the determining factor for DNAPL transport in clay aquitards, so DNAPL migration in fractured clay had drawn much attention of scholars [11–14].

Clay aquitards formed under different geological conditions usually present different structural characteristics and hydraulic properties. The reported fractured clay aquitards are generally composed of stiff Pleistocene (Q_3) deposits, which underwent a desiccation cracking process at late Q_3. The coastal areas of Southeast Asia is widely distributed the marine soft clay formed in Holocene (Q_4), which includes Ariake (Japan), Bangkok (Thailand), Busan (South Korea), Singapore, Mekong River Delta (Vietnam), and China's coastal areas [15]. The marine soft clays are generally homogenous deposits characterized with large void ratio (over 1.0) and flocculated structure [16]. Up to now, the characteristics and mechanisms of the DNAPL contamination in the marine clays were rarely reported. The efficiency of these marine sediments to protect the underlying aquifer against DNAPL contamination is still unclear.

China's coastal areas underwent intensive industrial development since the 1950s; numerous manufacture factories for electrical appliance, pharmaceutical, pesticide, printing, dyeing, and other purposes were constructed in the areas. Although most factories in these areas were shut down or moved to inland after the 2000s, potential contamination might have occurred during the operation of the plants. In this study, a chlorinated hydrocarbon (1,1,2-trichloroethane, DNAPL) contaminated site of a former pharmaceutical factory in Shanghai was introduced, and the mechanism of DNAPL migration in the marine soft clay was analyzed, characterized, and discussed herein.

2. Geological Settings

2.1. Holocene Transgression and Deposition of Marine Soft Clay. In early Holocene (Q_4^1, about 10,000 years ago), the climate became warmer and the sea level rose. This geological event is known as the Holocene transgression. In the middle Holocene (Q_4^2, about 5000 years ago) period, the transgression reached its peak in the southeast coastal areas in China (see Figure 1). Then, the coastal lines gradually retreated to current position. During this transgression-regression cycle, fine particles delivered by some rivers (Yellow River, Yangtze River, and Pearl River) sedimented in the coastal areas shown in Figure 1. The total thickness of the marine sediments generally ranged from 10.0 m to 30.0 m, increasing from the mainland to the coastline. These sediments usually have water content larger than liquid limit (w_L) and void ratio (e) lager than 1.0. Because of aging effect, they have larger intact shear strengths (most in the range of 30 to 45 kPa) than most modern marine clay. However, the remolded strength is low (most below 10 kPa), so they are categorized as marine soft clay in Chinese standard (Code for Investigation of Geotechnical Engineering, GB50021 2001).

Shanghai is located on the delta of Yangtze River, north of Hangzhou (HZ) Bay (see Figure 1). The ground is flat and the elevation is only several meters above the sea level. The groundwater level varies from 0.5 m to 1.5 m in depth annu-

Figure 1: Holocene transgression and marine soft clay distributions in China's coastal areas.

ally. The total thickness of the Quaternary sediments reaches 300.0 m, composed of various saturated clay, silt, and sand. These sediments constitute five (5) aquifers confined by the clayey aquitards. The overlying 25.0 m thick marine soft clays constitute the aquitard of the first aquifer right below the ground. The sedimentary environment and geotechnical properties of the Shanghai soft clays have been documented in some literature [15, 17]. The e ranges from 1.0 to 1.5 and the water content (w) range from 35% to 55%. Illite and illite/smectite mixtures are the predominant clay minerals, quartz, feldspar, mica, and carbonate prevail in nonclay minerals, the silt particle makes up over 60%, the clay content is usually below 30%, and the organic contents are below 2%, and the activities are generally around 0.8. These soils have liquid limit w_L below 45% and plasticity index I_P below 25, classified as low plasticity clay according to the unified soil classification system [18]. According to the Chinese standard [19], these soft clays are further categorized as soft silty clay ($10 \leq I_P < 17$) and soft clay ($I_P \geq 17$). The soft silty clay has lower clay content and smaller I_P than soft clay.

2.2. Soil Strata at the Site. The studied site was previously used as a pharmaceutical factory, which was built in 1958 and shut down in 2000. The ground is flat with the ground elevation of about 3.6 masl (meters above sea level). The groundwater level is about 1.0 m deep below the existing grade. The site location is shown in Figure 2.

Figure 3 illustrates the soil strata and the corresponding physical properties across the site. The physical properties were tested according to the China's National Standard for Geotechnical Testing Method (GB/T 50123-2019). From the ground surface to 36.0 m beneath the site, there were a total of six (6)
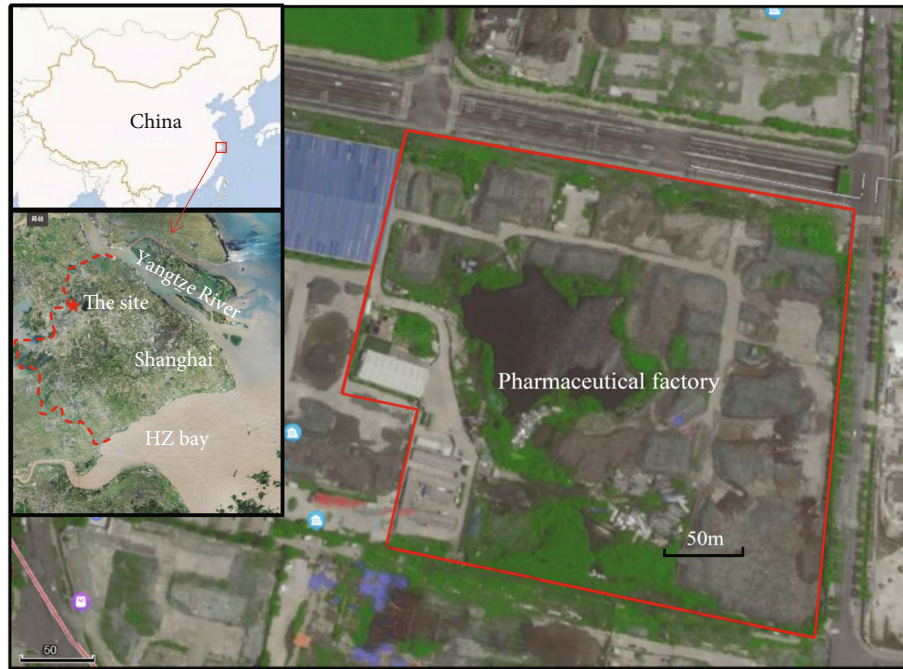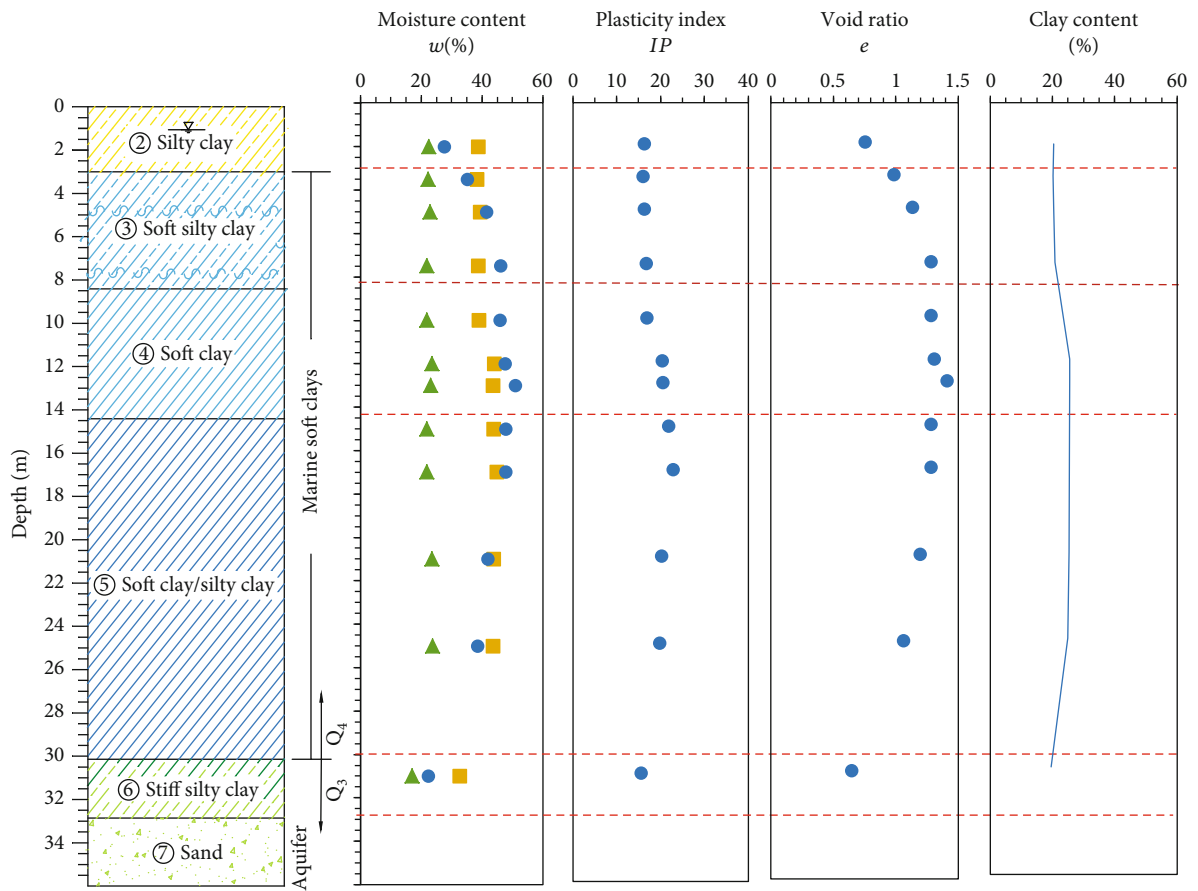
FIGURE 2: Site location plan.

FIGURE 3: Soil strata and physical characteristics.

FIGURE 4: Factory plan and contaminant distribution.

continuous soil strata with a minor elevation variation, except layer ⑥ which was absent at some areas. The soil strata are presented below:

Modern Deposit

(i) Layer ②, about 2.2 m thick, continuous silty clay with an average void ratio of 0.90, with desiccation fractures due to the weathering

Q_4 Marine Soft Clay

This consists of three (3) layers with total thickness about 25 m, void ratio 1.00-1.50, and hydraulic conductivities in the order of 10^{-7} cm/s.

(i) Layer ③, soft silty clay with average void ratio of 1.15, about 4.4 m thick, deposited in the regression process

(ii) Layer ④, soft clay with average void ratio of 1.40, largest I_P and highest clay content, about 4.4 m thick, deposited in the transgression process

(iii) Layer ⑤, soft clay/silty clay with average void ratio of 1.20, about 16.0 m thick, clay content and I_P decreased with the increase of depth, deposited in the transgression process

Q_3 Deposites

(i) Layer ⑥, dark green silty clay, hard, 3.0 m thick with average void ratio of 0.71

(ii) Layer ⑦, sand, the first aquifer of the site (saturated), not penetrated

3. Contaminant Distributions and Transport Patterns

3.1. Distributions of Contaminants. Layout of the former pharmaceutical factory is shown in Figure 4. A preliminary investigation conducted in 2014 prevailed that the manufacturing area had been seriously contaminated by volatile organic compounds (VOCs). Detailed investigation was further conducted in 2019, in which both shallow and deep boreholes were advanced to depths of 3.0 m-25.0 m at the manufacturing area. Boreholes over 15.0 m are plotted in Figure 4. All the soil samples were screened using a portable PID upon retrieval, and the contaminated samples were transported to the laboratory for chemical testing.

The distributions of the contaminants are illustrated in Figure 4. It showed that VOC contamination was detected in the north, middle, and south of the manufacturing area and semivolatile organic compound (SVOC) contamination was detected in the south. The organic contaminants were mainly chlorinated hydrocarbons, dominated by 1,1,2-trichloroethane ($C_2H_3Cl_3$), reaching several thousand mg/L in the soil samples. The physical and chemical properties

TABLE 1: Properties of 1,1,2-trichloroethane (20°C).

Organic contaminant	Relative dielectric constant	Water solubility (mg/L)	Density (g/cm³)	Viscosity (cP)	Surface tension (mN/m)	Relative octanol-water partition coefficient (log K_{ow})
1,1,2-Trichloroethane	7.52	4360	1.435	1.69	29.7	2.17

of the 1,1,2-trichloroethane are shown in Table 1. It is a DNAPL (density 1.435 g/cm³) with low water solubility (4.360 g/L) and low dielectric constant. Other detected chlorinated hydrocarbons included vinyl chloride (C_2H_3Cl), trichloroethylene (C_2HCl_3), and 1,2-dichloroethane ($C_2H_4Cl_2$), with total concentration below 200 mg/kg in the soil samples.

Most VOC contamination was found 7.0 m below grade and deeper, up to 22.0 m deep in layer ⑤, indicating a typical deep DNAPL contamination. Figure 5 shows the tested concentrations of 1,1,2-trichloroethane at three boreholes BH#60, BH#64, and BH#65 located in the central zone. The concentration C referred to the mass of 1,1,2-trichloroethane in per kilogram of wet soil (water-saturated soil in this case). At the depth from 3 m to 16 m, the 1,1,2-trichloroethane significantly exceeded 2.8 mg/kg, the limit defined in local bylaw. The contamination peaked at the depth around 10.0 m, where it was the interface between layers ③ and ④, with the concentrations over 2,000 mg/kg. The concentrations in layer ⑤, with depth exceeding 16 m, were mostly less than 2.0 mg/kg.

3.2. Presence of Pure 1,1,2-Trichloroethane.

NAPL in saturated soil presents in the forms of the aqueous phase (dissolved in pore water), adsorbed phase (adsorbed by solid components), and nonaqueous phase (pure NAPL). The aqueous phase migrates in/with pore water by convection and diffusion, while the nonaqueous phase migrates following the principle of two-phase flow [14]. The soil chemical analysis provided the total chemical concentration but was not capable to determine the proportions of the aqueous, sorbed, or nonaqueous phases. In this case study, the most testing results were less than 2,500 mg/kg and mass percent less than 0.25%. The saturation S_r of the pure 1,1,2-trichloroethane (if present), defined by the ratio of the volume of the pure 1,1,2-trichloroethane to the total pore volume of the soil, was within 5.5‰ (taking void ratio $e = 1.2$, porosity $n = 0.545$, and bulk density of soil $\rho = 1.73$ g/cm³). For such a small fraction, it is very difficult to identify the pure NAPL by direct methods [20].

Therefore, the partitioning calculation method described by Feenstra et al. [21] was used to identify the presence of pure NAPL (1,1,2-trichloroethane). Parker et al. [22] provided more details on this method. The principle of this method is to calculate the threshold concentration content C_s (unit in mg/g) first, which represents the maximum concentration in soil without pure NAPL. Thus, a tested concentration C greater than this threshold concentration C_s infers the existence of pure NAPL in soil. The threshold concentration C_s is calculated as follows, by assuming the aqueous phase reaching the effective solubility and the adsorption
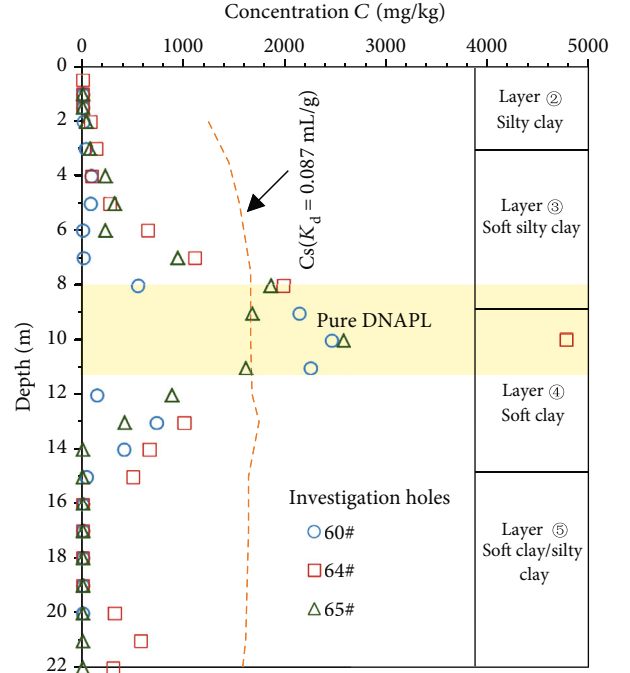

FIGURE 5: Profiles of 1,1,2-trichloroethan concentrations versus depths.

reaching equilibrium:

$$C_s = \frac{C_{ws}^e n}{\rho_{bwet}} + \frac{C_{ws}^e \rho_b K_d}{\rho_{bwet}} = \frac{(n + \rho_b K_d)C_{ws}^e}{\rho_{bwet}}, \quad (1)$$

$$\underbrace{\qquad}_{\text{dissolved}} \quad \underbrace{\qquad}_{\text{sorbed}}$$

where C_{ws}^e is the effective solubility of the NAPL in water (mg/L), K_d is the distribution coefficient between pore water and soil solids (mL/g), ρ_b is the soil dry bulk density (g/cm³), ρ_{bwet} is the soil wet bulk density (g/cm³), and n is the soil porosity. For single NAPL condition, the effective solubility C_{ws}^e can take the water solubility of the studied NAPL directly, which can be obtained from some literature [23]. For NAPL mixtures, the effective solubility of the studied NAPL should be determined with the mole fraction in the mixtures according to the Raoult's law as follows [21]:

$$C_{ws,i}^e = X_i C_{ws,i}, \quad (2)$$

where X_i is the mole fraction of the studied component i in the mixtures and $C_{ws,i}$ is the water solubility of the studied component i. It can be seen that the effective solubility of a NAPL in a mixture is smaller than its water solubility.

Most interesting NAPLs in soil contamination are nonpolar organics. The sorption of nonpolar organics in soils is predominantly the result of the partitioning of the dissolved chemicals from the groundwater onto the solid organic materials in the soil. The partition coefficient K_d in Equation (1) is defined as Zheng and Gordon [23]:

$$K_d = f_{oc} K_{oc}, \tag{3}$$

where K_{oc} is the organic carbon-water partition coefficient for the chemical of interest and f_{oc} is the fraction of organic carbon in the soil.

An empirical equation proposed by Kenaga and Goring [24] is used to estimate the K_{oc} from the water solubility (C_{ws}) as follows:

$$\text{Lg}(K_{oc}) = -0.55 \lg (C_{WS}) + 3.64, \tag{4}$$

where the K_{oc} is in mL/g and the C_{ws} is in mg/L. The C_{ws} of the 1,1,2-trichloroethane is 4360 mg/L. The K_{oc} of 1,1,2-trichloroethane estimated by Equation (4) is $K_{oc} = 43.54$ mL/g. The f_{oc} of the marine soft clays (layers ③, ④, and ⑤) measured by the potassium dichromate oxidation spectrophotometric method varies from 0.10% to 0.20%. Taking $f_{oc} = 0.2\%$ (measured maximum value) and $K_{oc} = 43.54$ mL/g, the K_d determined by Equation (3) is 0.087 mL/g.

To simplify the analysis, single 1,1,2-trichloroethane was considered because its concentrations and mole fractions were much higher than that of other chlorinated hydrocarbons (vinyl chloride, trichloroethylene, and 1,2-dichloroethane) detected in soil. The water solubility C_{ws} of the 1,1,2-trichloroethane was taken as the effective solubility C_{ws}^e in Equation (1), i.e., $C_{ws}^e = 4,360$ mg/L. Taking $K_d = 0.087$ mL/g and the measured n, ρ_b, and ρ_{bwet} at each depth into Equation (1), the resulting threshold concentration C_s is shown in Figure 5. Tested concentrations over this threshold infer the presence of pure 1,1,2-trichloroethane. It was evident that the concentrations at the depth of 8.0 m-11.0 m exceeded the threshold value of C_s (around 1700 mg/g) and would lead to the conclusion that pure 1,1,2-trichloroethane was present at this depth.

3.3. Transport Velocity. The presence of pure 1,1,2-trichloroethane can also be confirmed by the analysis of transport velocity. It is well known that the aqueous phase of the chemical migrates in/with pore water by convection and/or diffusion. Under the condition of limited/minimum downward seepage in the low permeability sediments, the convection can be neglected, and the molecular diffusion is the only dominating factor [14]. Under this condition, the velocity of molecular diffusion is determined by the effective molecular diffusion coefficient of the chemical, which is in the order of magnitude of 10^{-10}-10^{-9} m^2/s for most organic contaminates. Due to the great thickness and low permeability of the marine soft clays in this studied case, the downward seepage velocity caused by water extraction from the underlying aquifer is assumed to be in the order of 1.0 cm/year. According to the analysis by Parker et al. [6], the diffusive velocity is only a few centimeters per year. Literally, it will

take several hundred years to diffuse the aqueous phase of 1,1,2-trichloroethane to 10.0 m deep; this is inconsistent with the fact that the 1,1,2-trichloroethane transported downward at least 10.0 m deep within sixty-one (61) years.

The two-phase flow involves the NAPL-water retention relationship, and it usually needed to be analyzed with numerical modeling method. Due to the higher density and low viscosity, pure DNAPL is prone to move much faster through the soil pores than the dissolved phase [12]. Gao et al. [25] have conducted two-dimensional two-phase flow analysis to study the DNAPL transport in similar soft clay using COMSOL, a multiphase analysis program. The analysis program revealed that even with the minimum presents of small pore/fracture in the soil, the factual velocity of the pure DNAPL flow can reach tens of centimeters per year, much larger than the Darcy velocity (volume averaged velocity). This explained the fact that the 1,1,2-trichloroethane transported downward more than 10.0 m within sixty-one (61) years across the study area. The aqueous phase 1,1,2-trichloroethane detected in the lower portion of layers ④ and ⑤, with concentration less than the threshold value, was likely due to the dissolution of the pure phase.

4. Mechanisms of DNAPL Deep Migration

Field investigations clearly demonstrated that pure DNAPL might migrate to a great depth in the marine soft clays. As macroscopic preferential pathways, e.g., desiccation fractures, visible macrofractures, and root holes were not found in the retrieved soil samples, the pore networks related to soil structures are probably the pathways of the DNAPL migration.

Contamination of clay by petroleum substances or other organic fluids, characterized by lower dielectric constant than water, might change the structures, physical properties, and mechanical properties of soils [26–32]. When organic fluids seeped or mixed with the clayey soil, a "sandy effect" characterized by clay particle aggregation developed, which would decrease the plasticity and increase the permeability of soil to a great extent. The relative dielectric constant of 1,1,2-trichloroethane was 7.52, much less than that of water (78.36). Therefore, change of soil properties by NAPL-clay interactions was a possible mechanism leading DNAPL to transport to 22.0 m deep. To verify this assumption, contaminated and uncontaminated soil samples collected from two boreholes were tested and compared. Both the uncontaminated samples and contaminated samples were collected at the same depths, 3.0 m, 6.0 m, 12.0 m, and 17.0 m in layers ②, ③, ④, and ⑤, respectively. The contaminated and uncontaminated soil samples presented the same colour and other appearances, except for the odour in the contaminated samples.

4.1. Changes of Soil Properties. Atterberg limit tests and permeability tests were conducted on both UC (uncontaminated) and C (contaminated) samples, according to China's National Standard for Geotechnical Testing Method (GB/T 50123-2019). The Atterberg limits were determined by the falling cone methods. The measured liquid limit w_L,

plastic limit w_P, and plasticity index I_P of the two types of samples are shown in Table 2. It can be seen in Table 2 that the values of liquid limit w_L, plastic limit w_P, and plasticity index I_P were almost the same for UC and C samples, inferring that the contamination exerted a minimum impact to the physical properties of these soils.

The hydraulic permeability of the two types of samples was determined by falling head hydraulic conductivity tests. Three hydraulic conductivity tests were conducted on both vertically and horizontally trimmed samples for each stratum, to obtain the vertical and horizontal hydraulic conductivity k_v and k_h, respectively. The average hydraulic conductivities of each stratum are shown in Table 3. The vertical hydraulic conductivity k_v of the contaminated soil increased to a certain extent, and the ratio of k_v (C)/k_v (UC) was within the order of 2.0. The changes of horizontal hydraulic conductivity k_h were more complex, but the ratio of k_h (C)/k_h (UC) was also within 2.0. It seems there are correlations among the contamination degree, soil plasticity, and the changes of permeability. The upmost layer ② undergoing most severe contamination (although the current concentration is low) and the layer ④ having larger soil plasticity and larger contamination changed more significant than layers ③ and ⑤.

Compared to the reported dramatic (up to several orders) decrease in soil plasticity and increase in hydraulic conductivity observed on laboratory-contaminated samples [26–32], the change of soil properties of these field-contaminated samples was limited. The reason may attribute to the low content of the organic contaminant in the soil samples. The mass percent of the contaminant is most less than 0.25%, much smaller than the laboratory-contaminated samples prepared with sedimentation method (settling soil in pure DNAPL) or penetration method (penetrating pure DNAPL into soil under a certain pressure).

4.2. Pore Structures. The pore in soil is the space for transport and accommodation of the contaminants, so the pore structure could affect the transporting behavior. Mercury intrusion porosimetry (MIP) tests were carried out to obtain the pore size distributions of layers ③, ④, and ⑤. For each stratum, one (1) UC and one (1) C soil samples were tested, respectively. The soil samples were trimmed into small sticks, quickly frozen in Freon 22, freeze fractured, and sublimated as suggested by Delage and Lefebvre [33]. A Micromeritics Corp. porosimeter (type Autopore 9620) was used for mercury intrusion porosimetry test, which allowed the pressures as high as 430 MPa and the invaded pore size as small as 0.0029 μm. Figures 6–8 show the incremental pore volume dV (in mL/g, pore volume in unit soil mass in dry weight) versus pore diameter d relationships of the three strata. The pore sizes were divided into five (5) levels, and the pore volume (in mL/g) and the percent content of each level are also calculated and shown in Figures 6–8.

The three strata exhibited different pore structures. The dV versus d relationships of layer ③ (silty clay) show an obvious bioporous structure, with the first peak at 0.1 μm $< d < 1\,\mu$m and the second peak at 10 μm $< d < 40\,\mu$m. The two levels of pores accounted for about 40% of the pore vol-

TABLE 2: Atterberg test results for UC and C soil samples.

Soil stratum	Liquid limit w_L (%)		Plastic limit w_P (%)		Plasticity index I_P (%)	
	UC	C	UC	C	UC	C
Layer ②, silty clay	38.9	38.5	22.6	22.4	16.3	16.1
Layer ③, silty clay	39.4	38.8	23.1	22.1	16.3	16.7
Layer ④, clay	44.2	43.8	23.8	23.3	20.4	20.5
Layer ⑤, clay/silty clay	43.8	44.0	23.9	23.7	19.9	20.3

ume, respectively. This bioporous structure was not predominant in layers ④ and ⑤. For layer ④ (clay), the peak was in the range of 1 μm $< d < 4\,\mu$m, accounting for half of the total volume; for layer ⑤ (clay/silty clay), the peak was in the range of 0.1 μm $< d < 1\,\mu$m, accounting for 40% to 60% of the total volume. The measured average pore diameter (= 4V/A, V is the total pore volume and A is the total pore area) was 0.32 μm for layer ③ and 0.10 μm for layers ④ and ⑤. These results showed that although layer ③ had the smallest void ratio, it presented a more open structure than layers ④ and ⑤.

The primary structures of the soils were determined by the components of the sediments and the depositional environment. The marine soft clay generally presents flocculated structure due to the salt-water environment [16, 33, 34]. The pore size below 0.4 μm belongs to the introaggregate pore, while the pore size over 0.4 μm belongs to the interaggregate pore [33, 35]. Higher proportion of large interaggregate pores ($d > 10\,\mu$m) in layer ③ was likely resulted from the higher silt content (over 70%), which could form a granular-link bound structure and large interparticle pores [34]; layer ④ exhibited higher content of interaggregate pores than layer ⑤, indicating a more flocculated structure than layer ⑤. The different soil structures and pore size distributions of the three marine soft clays may influence the transport of DNAPL, which will be discussed in detail later.

In laboratories, there are many evidence that decreasing the dielectric constant of pore liquid may lead to strong aggregation of clay particles. However, available field findings are yet limited. Dorota and Jerzy [36] have reported enhanced aggregation and increased macropores in a clay stratum contaminated by gasoline, in which the concentrations exceed 5.000 mg/kg. Figures 6–8 show that the content of large pores with $d > 10\,\mu$m tended to increase in contaminated soils, indicating a tendency of aggregation by NAPL-soil interactions. However, due to the natural variability of soil structures and the limited test data, this aggregation effect cannot be confirmed in this study. Generally speaking, the contaminated and uncontaminated soils have the similar pore structures, so it can be concluded that the primary structure of the soil does not change dramatically by the contamination.

4.3. Influence of Pore Structure on DNAPL Transport. According to the theory of two-phase flow in a porous material, the capillary pressure p_c determines the transport velocity and the NAPL saturation (S_r, the ratio of NAPL volume

TABLE 3: Hydraulic conductivities (k) for UC and C soil samples.

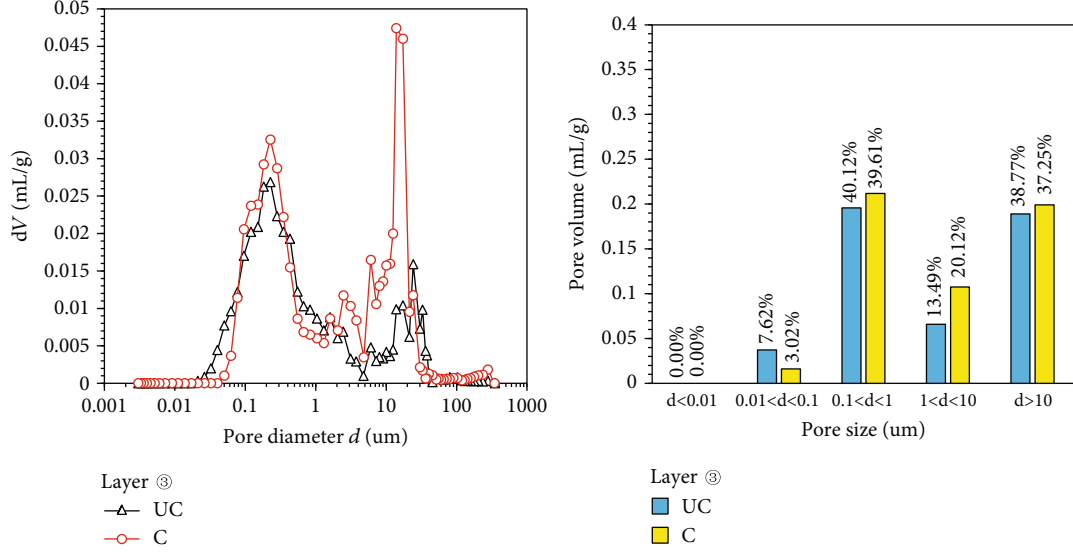| Soil stratum	k_h (10^{-7} cm/s)		k_h (C)/k_h (UC)	k_v (10^{-7} cm/s)		k_v (C)/k_v (UC)
	UC	C		UC	C	
Layer ②, silty clay	2.32	3.01	1.3	1.62	2.94	1.81
Layer ③, silty clay	5.24	6.37	1.2	6.37	5.33	0.84
Layer ④, clay	0.83	1.67	2.0	0.81	0.87	1.07
Layer ⑤, clay/silty clay	1.73	1.84	1.06	1.61	1.78	1.11

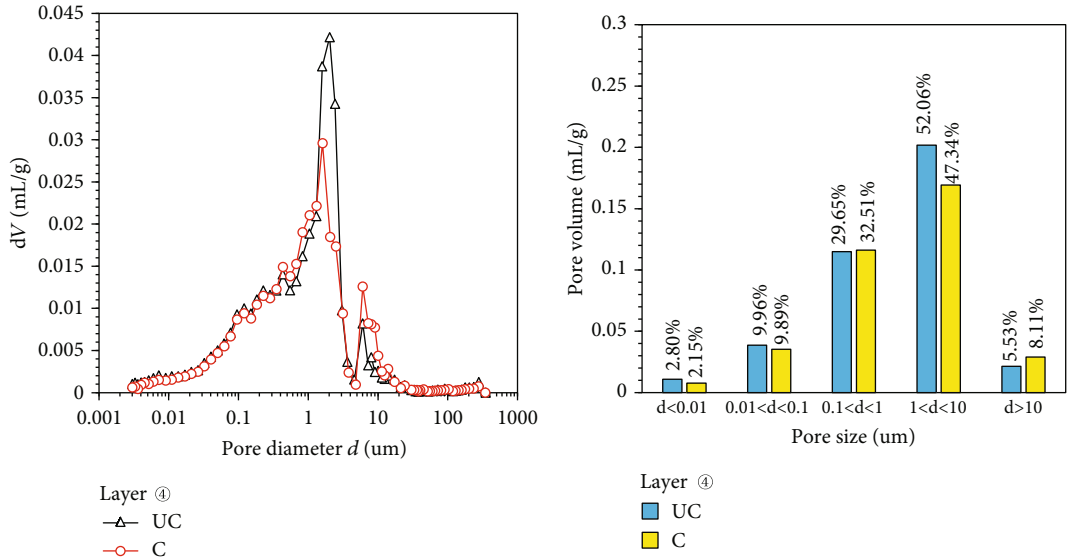FIGURE 6: Pore size distributions in layer ③ (soft silty clay).

FIGURE 7: Pore size distributions in layer ④ (soft clay).

to the total pore volume) in saturated soil. The capillary pressure p_c in a NAPL-water system is expressed as follows:

$$p_c = p_N - p_w, \qquad (5)$$

where p_N is nonaqueous liquid pressure and p_W is the pore water pressure. NAPL displaces pore water under a p_c until an equilibrium S_r is reached. The invaded pore diameter under a specific p_c can be estimated by the capillary model
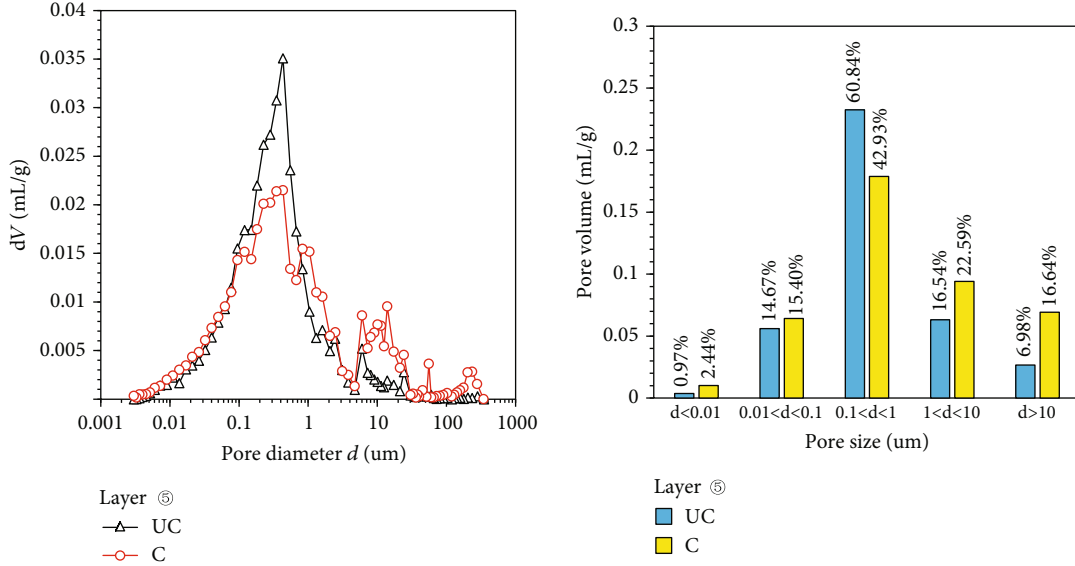
FIGURE 8: Pore size distributions in layer ⑤ (soft clay/silty clay).

as follows [37]:

$$d = \frac{4\sigma \cos \theta}{p_c} = \frac{4\sigma \cos \theta}{p_N - p_W}, \tag{6}$$

in which d is the invaded pore diameter, σ is the interfacial tension between the nonaqueous liquid and water (dyne/cm), and θ is the contact angle measured through the water.

According to Equation (6), water in large pore is displaced by DNAPL first; then, water in small pore is gradually displaced with the increase of p_c. The interfacial tension between the 1,1,2-trichloroethane and water, σ, is 29.7 mN/m [38]. No measured contact angles for 1,1,2-trichloroethane and water-saturated natural clays were found in the literature; however, measured values for similar chlorinated solvent DNAPLs (chloroform and carbon tetrachloride) range from 27° to 31° [39]. Here, the contact angle θ was taken as 29°. Substituting these parameter values into Equation (6), at the p_c of 5.0 kPa and 10.0 kPa (a conservative value in most cases), the invaded pore diameters are 20.8 μm and 10.4 μm, respectively.

This simple analysis reveals the possibility of the transport of the pure 1,1,2-trichloroethane through the pores with diameter of tens of microns or greater, provided that the displacement pressure head reaches tens of centimeters. O'Hara et al. [13] conducted laboratory experiments on a column of naturally fractured clay to demonstrate the entry and rapid flow of TCE (DNAPL), showing that DNAPL with 30 cm displacement pressure head entered fractures with apertures of 17 μm or greater. Therefore, the pores greater than tens of microns are likely the pathway of the migration of 1,1,2-trichloroethane in the soil.

The proportion of large interaggregate pores with $d > 10 \mu$m in each layer is summarized in Table 4, which were further divided into three levels, $d > 10 \mu$m, $d > 20 \mu$m, and $d > 50 \mu$m. It is evident that these large pores took a certain

TABLE 4: Proportion of large interaggregate pores ($d > 10 \mu$m).

Soil stratum	Volumetric proportion (%)					
	$d > 10 \mu$m		$d > 20 \mu$m		$d > 50 \mu$m	
	UC	C	UC	C	UC	C
Layer ③, silty clay	38.1	35.6	31.4	11.2	15.9	2.3
Layer ④, clay	4.9	7.0	2.6	2.5	1.7	1.5
Layer ⑤, clay/silty clay	6.4	16.3	4.5	7.5	1.8	4.2

proportion in these marine soft clays. In the silty clay of layer ③, the pores with $d > 10 \mu$m accounted for one-third. This is possible the reason that the 1,1,2-trichloroethane could penetrate this layer. Although the void ratio of layer ④ (clay) was greater than that of layer ③ (silty clay), the proportion of pores with $d > 10 \mu$m is much less than that of layer ③. This can explain why the hydraulic conductivity of layer ④ was much smaller than that of layer ③ (see Table 3) and why DNAPL accumulated at the top of layer ④. However, the content of pores of $d > 10 \mu$m in layer ④ still exceeded 5%, so this layer was not functioned as an effective barrier to prevent the downward movement of DNAPL. If no measures are taken, the DNAPL will probably continue to migrate downward, until reaching the layer ⑤. Layer ⑤ has a larger proportion of large pores ($d > 10 \mu$m) than layer ④, consistent with its relatively lower plasticity and lower clay content. Therefore, DNAPL can also penetrate the layer ⑤ and contaminate the underlying aquifer eventually.

The large interaggregate pores in the marine soft clay play a similar role with those fractures in the fractured clay. They both provide the preferential pathways of the transport of DNAPL in the clayey soil. The proportion of large interaggregate pores in marine soft clay is mainly determined by the primary structure which is related to the sedimentary environments. Different sedimentary environments could

result in different pore structures, such as the three strata in the studied site. For fractured clays, the desiccation cracks or shear fractures generally formed in the postsedimentary environments. The migration of contaminants in fractures is controlled by the fracture aperture, spacing, and orientation. The depth of the vertically developed fractures determines the depth that DNAPL can reach. The entry pressures for the two types of preferential pathways are different. Theoretically, the entry pressure for a parallel-plate geometry is half of that for a cylindrical-tube geometry with the same size.

5. Conclusions

A site contaminated with organic chemicals was studied in detail in this study, where deep 1,1,2-trichloroethane (DNAPL) contamination was detected in marine soft clays characterized as flocculated structure and large void ratio. Some fundamental knowledge about the DNAPL contamination in this type of soil based on some simple analysis is summarized as follows: pure DNAPL invaded and transported downward in the marine soft clays following the principle of two-phase flow, accumulated at the interface between the upper soft silty clay (layer ③) and lower soft clay (layer ④). The vertical transport velocity is considerable, reaching to depth 22.0 m below the ground surface within sixty-one (61) years. The contamination (most below 2500 mg/kg) impacts the soil properties slightly: the Atterberg limits remained unchanged, while the hydraulic conductivities increased within twofold. The NAPL-clay interaction is not the reason leading to the deep contamination.

The primary pore structures well explain the mechanism of transport and distribution of the contaminant in soil. The large interaggregate pores ($d > 10\,\mu$m) in the open flocculated structure were believed to be pathways for pure DNAPL migration in the marine soft clays. The proportion of the large interaggregate pores ($d > 10\,\mu$m) was found to increase with the decrease of soil plasticity and clay content. Considering the characteristics of soil structures, the marine soft clays cannot constitute a barrier to the downward migration of pure DNAPL.

Data Availability

The test data used to support the findings of this study are included within the article.

Conflicts of Interest

Acknowledgments

References

[1] H. I. Essaid, B. A. Bekins, and I. M. Cozzarelli, "Organic contaminant transport and fate in the subsurface: evolution of knowledge and understanding," *Water Resources Research*, vol. 51, no. 7, pp. 4861–4902, 2015.

[2] G. Ponzini, G. Crosta, and M. Giudici, "The hydrogeological role of an aquitard in preventing drinkable water well contamination: a case study," *Environmental Health Perspectives*, vol. 83, no. 3, pp. 77–95, 1989.

[3] U.S. EPA, *Guidelines for Delineation of Wellhead Protection*, Areas US. Environmental Protection Agency, Office of Ground-Water Protection, Washington D.C, 1987.

[4] J. A. Cherry, B. L. Parker, K. R. Bradbury et al., *Contaminant Transport through Aquitards: A "State of the Science" Review*, Colorado, AWWA Research Foundation, Denver, 2006.

[5] M. Filippini, B. L. Parker, E. Dinelli, P. Wanner, S. W. Chapman, and A. Gargini, "Assessing aquitard integrity in a complex aquifer - aquitard system contaminated by chlorinated hydrocarbons," *Water Research*, vol. 171, article 115388, p. 12, 2020.

[6] B. L. Parker, J. A. Cherry, and S. W. Chapman, "Field study of TCE diffusion profiles below DNAPL to assess aquitard integrity," *Journal of Contaminant Hydrology*, vol. 74, no. 1-4, pp. 197–230, 2004.

[7] R. J. Roberts, J. A. Cherry, and F. W. Schwartz, "A case study of a chemical spill: polychlorinated biphenyls (PCBs): 1. History, distribution, and surface translocation," *Water Resources Research*, vol. 18, no. 3, pp. 525–534, 1982.

[8] F. W. Schwartz, J. A. Cherry, and J. R. Roberts, "A case study of a chemical spill: polychlorinated biphenyls (PCBs): 2. Hydrogeological conditions and contaminant migration," *Water Resources Research*, vol. 18, no. 3, pp. 535–545, 1982.

[9] Industries, P.P.G, *Phase 2*, Draft Site Wide RCRA Facility Investigation. U.S EPA, 1995.

[10] A. S. Fjordbøge, G. S. Janniche, T. H. Jørgensen et al., "Integrity of clay till aquitards to DNAPL migration: assessment using current and emerging characterization tools," *Groundwater Monitoring & Remediation*, vol. 37, no. 3, pp. 45–61, 2017.

[11] P. R. Jørgensen, M. Hoffmann, J. P. Kistrup, C. Bryde, R. Bossi, and K. G. Villholth, "Preferential flow and pesticide transport in a clay-rich till: field, laboratory, and modeling analysis," *Water Resources Research*, vol. 38, no. 11, pp. 28-1–28-15, 2002.

[12] B. H. Kueper and D. B. Mcwhorter, "The behavior of dense, nonaqueous phase liquids in fractured clay and rock," *Groundwater*, vol. 29, no. 5, pp. 716–728, 1991.

[13] S. K. O'Hara, B. L. Parker, and P. R. Jørgensen, "Trichloroethene DNAPL flow and mass distribution in naturally fractured clay: evidence of aperture variability," *Water Resources Research*, vol. 36, no. 1, pp. 135–147, 2000.

[14] B. L. Parker, J. A. Cherry, and P. Wanner, "Determining effective diffusion coefficients of chlorohydrocarbons in natural clays: unique results from highly resolved controlled release field experiments," *Journal of Contaminant Hydrology*, vol. 250, 2022.

[15] C. J. Wu, G. L. Ye, L. L. Zhang, D. Bishop, and J. H. Wang, "Depositional environment and geotechnical properties of Shanghai clay: a comparison with Ariake and Bangkok clays," *Bulletin of Engineering Geology & the Environment*, vol. 74, no. 3, pp. 717–732, 2015.

[16] J. K. Mitchell, *Fundamentals of Soil Behavior*, John Wiley & Sons Inc, New York, 1993.

[17] D. Z. Gao, D. D. Wei, and Z. X. Hu, "Geotechnical properties of Shanghai soils and engineering applications," in *Marine Geotechnology and Nearshore/Offshore Structures*, R. C. Chaney and H. Y. Fang, Eds., pp. 161–177, American Society for Testing and Materials, Philadephia, 1986.

[18] ASTM, "Standard practice for classification of soils for engineering purposes (unified soil classification system)," 2017.

[19] Ministry of construction of China, *Code for investigation of geotechnical engineering*, China Architecture & Building Press, Shanghai, 2002.

[20] T. W. Griffin and K. W. Watson, "A comparison of field techniques for confirming dense nonaqueous phase liquids," *Ground Water Monitoring & Remediation*, vol. 22, no. 2, pp. 48–59, 2002.

[21] S. Feenstra, D. M. Mackay, and J. A. Cherry, "A method for assessing residual NAPL based on organic chemical concentrations in soil samples," *Ground Water Monitoring & Remediation*, vol. 11, no. 2, pp. 128–136, 1991.

[22] B. L. Parker, J. A. Cherry, S. W. Chapman, and M. A. Guilbeault, "Review and analysis of chlorinated solvent dense nonaqueous phase liquid distributions in five sandy aquifers," *Vadose Zone Journal*, vol. 2, no. 2, pp. 116–137, 2003.

[23] C. M. Zheng and D. B. Gordon, *Applied Contaminant Transport Modeling*, Higher Education Press, Beijing, 2009.

[24] E. Kenaga and C. A. I. Goring, "Relationship between water solubility, soil sorption, octanol-water partitioning, and concentration of chemicals in biota," in *Aquatic Toxicology*, p. 78, ASTM International, 1980.

[25] Y. B. Gao, S. B. Zhang, and T. Li, "Numerical analysis of vertical migration of dense nonaqueous-phase liquids in saturated clay," *Journal of Tongji University (Natural Science)*, vol. 48, no. 1, pp. 24–32, 2020.

[26] D. Ayral, *Impact of Clay-DNAPL Interactions on the Transport of Chlorinated Solvents in Low Permeability Subsurface Zones*, University of Michigan, 2015.

[27] J. J. Bowders, *The Influence of Various Concentrations of Organic Liquids on the Hydraulic Conductivity of Compacted Clay. Geotechnical Engineering Dissertation GT85-2*, The University of Texas at Austin 218, 1985.

[28] K. W. Brown and J. C. Thomas, "A mechanism by which organic liquids increase the hydraulic conductivity of compacted clay materials," *Soil Science Society of America Journal*, vol. 51, no. 6, pp. 1451–1459, 1987.

[29] F. Fernandez and R. M. Quigley, "Hydraulic conductivity of natural clays permeated with simple liquid hydrocarbons," *Canadian Geotechnical Journal*, vol. 22, no. 2, pp. 205–214, 1985.

[30] A. Kaya and H. Y. Fang, "The effects of organic fluids on physicochemical parameters of fine-grained soils," *Canadian Geotechnical Journal*, vol. 37, no. 5, pp. 943–950, 2000.

[31] M. Khamehchiyan, A. H. Charkhabi, and M. Tajik, "Effects of crude oil contamination on geotechnical properties of clayey and sandy soils," *Engineering Geology*, vol. 89, no. 3–4, pp. 220–229, 2007.

[32] F. T. Madsen and J. K. Mitchell, "Chemical effects on clay farbric and hydraulic conductivity," *The Landfill*, vol. 20, pp. 201–251, 1989.

[33] P. Delage and G. Lefebvre, "Study of the structure of a sensitive Champlain clay and of its evolution during consolidation," *Canadian Geotechnical Journal*, vol. 21, no. 1, pp. 21–35, 1984.

[34] G. R. Gao, "Microfabric features, composition, and microstructure classification of marine soils in China," in *Marine Geotechnology and Nearshore/Offshore Structures*, R. C. Chaney and H. Y. Fang, Eds., pp. 178–195, American Society for Testing and Materials, Philadephia, 1986.

[35] C. Lapierre, S. Leroueil, and J. Locat, "Mercury intrusion and permeability of Louiseville clay," *Canadian Geotechnical Journal*, vol. 27, no. 6, pp. 761–773, 1990.

[36] I. M. Dorota and T. Jerzy, "Effects of petroleµm pollution on clay soil microstructure," *Geologija*, vol. 50, pp. 68–74, 2008.

[37] J. Bear, *Hydraulics of groundwater*, Dover Publication, New York, 1979.

[38] M. P. Andersson, M. V. Bennetzen, A. Klamt, and S. L. S. Stipp, "First-principles prediction of liquid/liquid interfacial tension," *Journal of Chemical Theory and Computation*, vol. 10, no. 8, pp. 3401–3408, 2014.

[39] R. M. Cohen and J. W. Mercer, *DNAPL site evaluation. Research report*, Geotrans, Inc.,Sterling, 1993.